Magnetic-Solar Hybrid Attitude Control of Satellites in Near-Equatorial Orbits

V. J. MODI* AND K. C. PANDE†
The University of British Columbia, Vancouver, Canada

Nutation damping using the Earth's magnetic field for spin-axis and solar radiation pressure for pitch control is studied for spacecraft in near-synchronous altitudes. The nonlinear, nonautonomous, coupled equations of motion involving a large number of parameters are only amenable to a numerical approach. The response data, presented as functions of the system parameters, show the controller's effectiveness in damping the most severe disturbances in a few degrees of the satellite's orbital travel. The controller provides versatility to the satellite, enabling it to change its preferred orientation in orbit and, hence, undertake diverse missions. The effectiveness of the system even in presence of rotor spin decay promises an increased satellite lifespan. An illustrative example using the inertia properties of Anik and the proposed Canadian Communications Technology Satellite demonstrates the feasibility of the concept in the geostationary orbit.

Nomenclature‡

A = total area of solar controller plates
$\bar{B}$ = geomagnetic induction vector
B_i, B_j, B_k / B_{xn}, B_{yn}, B_{zn} = components of $\bar{B}/D_m$ along the x, y, z and x_n, y_n, z_n axes, respectively
C, C_m = solar and magnetic parameters, respectively
D_m = geomagnetic dipole moment M_e/R^3, $M_e = 8.1 \times 10^{25}$ gauss-cm^3
I = inertia parameter, I_x/I_y
J = platform inertia fraction, I_{xp}/I_x
K = viscous damping parameter, $K_d(R_p{}^3/\mu)^{1/2}/I_y$
K_d = viscous damping coefficient
I_x, I_y, I_z = principal moments of inertia of the satellite
I_{xp} = moment of inertia of the platform about the axis of symmetry
$\bar{M}$ = magnetic torque vector
O = center of force
P = pericenter
$\bar{P}$ = applied magnetic dipole vector
P_g, P_m = geographic and geomagnetic polar axes, respectively
Q_i = generalized forces, $i = \gamma, \beta, \lambda$
$Q_\lambda{}^m, Q_\lambda{}^s$ = generalized forces in the λ degree of freedom due to magnetic and solar controllers, respectively
R = distance between the satellite center of mass and the center of force
R_p = distance between the pericenter and the center of force
S = center of mass of the satellite
S_i = switching functions, $i = \gamma, \beta, \lambda$
U, U_1, U_2 = polarities of the applied dipoles
e = eccentricity
h_z = constant of the motion
i, i_m = inclinations of the orbital plane from the ecliptic and equatorial planes, respectively
$\bar{i}, \bar{j}, \bar{k}$ = unit vectors along x, y, and z axes, respectively
m = controller gain
n_e, n_r = rates of rotation of the earth and the regression of the line of nodes, respectively
$\bar{p}, \bar{p}_1, \bar{p}_2$ = unit vectors specifying applied dipole orientations, $\bar{p} = p_i\bar{i} + p_j\bar{j} + p_k\bar{k}$
p_o = solar radiation pressure, 4.65×10^{-5} dynes/cm^2
t = time
$\bar{u}$ = unit vector in the direction of the sun, $u_i\bar{i} + u_j\bar{j} + u_k\bar{k}$
u_i = $\cos\phi(\sin\gamma\cos\beta\cos\eta + \sin\beta\sin\eta) + \sin\phi\{\cos i(\sin\gamma\cos\beta\sin\eta - \sin\beta\cos\eta) - \sin i\cos\beta\cos\gamma\}$
u_j = $\cos\phi\cos\gamma\cos\eta + \sin\phi(\cos i\cos\gamma\sin\eta + \sin i\sin\gamma)$
u_k = $\cos\phi(\sin\gamma\sin\beta\cos\eta - \cos\beta\sin\eta) + \sin\phi\{\cos i(\sin\gamma\sin\beta\sin\eta + \cos\beta\cos\eta) - \sin i\sin\beta\cos\gamma\}$
x, y, z = principal body coordinates
x_p, y_p, z_p = platform-fixed coordinate system
x', y', z' = inertial coordinates
x_o, y_o, z_o = rotating coordinate system with x_o normal to the orbital plane and y_o along the local vertical
x_1, y_1, z_1 / x_2, y_2, z_2 = intermediate body coordinates resulting from rotations γ and β about z_o and y_1 axes, respectively
x_n, y_n, z_n = inertial coordinate system with x_n normal to the orbital plane and y_n along the line of nodes referred to the equatorial plane
Φ = coning angle of the spin axis, $\cos^{-1}(\cos\beta\cos\gamma)$
Ω, Ω_m = angles between the vernal equinox and the line of nodes referred to the ecliptic and equatorial planes, respectively
$\alpha, \beta, \gamma, \lambda$ = attitude angles
$\beta_f, \gamma_f, \lambda_f$ = final orientation
β_m = longitude of the plane containing both the geographic and geomagnetic polar axes from the vernal equinox
δ = rotation of solar controller plates
ε = distance between the center of pressure of solar controller plates and the satellite center of mass
ε_m = geomagnetic polar axis declination, 11.4°
η, η_m = $\omega + \theta$ and $\omega_m + \theta$, respectively
θ = orbital angle
μ = gravitational constant
ρ, τ = reflectivity and transmissibility of solar control plates, respectively
τ_d = damping time
σ = spin parameter
ϕ = solar aspect angle, angle between the direction of the sun and the line of nodes referred to the ecliptic
ϕ_m = $\beta_m - \Omega_m$
ω, ω_m = angles between the line of apsides and the line of nodes referred to the ecliptic and the equatorial planes, respectively.

Received October 15, 1973; revision received July 29, 1974. The investigation was supported by the Federal Department of Communications Contract OGR2-0203.

Index category: Spacecraft Attitude Dynamics and Control.

* Professor, Department of Mechanical Engineering. Member AIAA.

† Post-Doctoral Fellow, Department of Mechanical Engineering. Student Member AIAA.

‡ Dots and primes indicate differentiation with respect to t and θ, respectively. The subscript o denotes initial condition.

Introduction

UTILIZATION of the normally destabilizing environmental forces for attitude control of satellites has received some attention in recent years. One of the possibilities of employing

these forces to advantage is through the interaction of onboard electromagnetic dipoles with the Earth's magnetic field. The concept appears to be particularly attractive because of improved reliability achieved by the elimination of moving parts. Wheeler[1] investigated the use of a single dipole along the spin axis for both attitude control and nutation damping. The analysis, however, considered the desired final orientation to be inertially fixed and the spin rate constant during the control maneuver. The first operational magnetically controlled satellites, the TIROS wheels, have been discussed by Hecht and Manger[2] and Lindorfer and Muhlfelder.[3] In a recent study, Shigehara[4] developed a control law based on the asymptotic stability criterion for the spin axis and the spin rate control using dipoles along the spin axis and perpendicular to it, respectively. Librational damping of a nonspinning satellite in the gravity field was considered by Bainum and Mackison[5] who applied the sample and hold concept to a system with three mutually perpendicular electromagnets. Although time constants of approximately one to two orbits for roll-yaw damping were attainable, the inadequacy of the system for pitch control in equatorial orbits, where the geomagnetic field is nearly parallel to the orbit normal, became apparent.

Another environmental force of interest has been the solar radiation pressure. Modi et al.[6-8] have proposed semi-passive solar controllers, for both gravity oriented and spinning satellites, which not only damp the satellite librations but also enable them to attain any arbitrary orientation in orbit. Scull[9] reported the experiment aboard Mariner IV spacecraft which demonstrated the effectiveness of the solar pressure controller operating in conjunction with active gyros.

This paper explores the feasibility of three-axis nutation damping and attitude control of satellites using a hybrid magnetic-solar control system. A general configuration consisting of a spinning rotor and a stabilized platform is selected which permits reduction to the case of nonspinning satellites. Two magnetic controller models are considered for orienting the spin axis while the solar radiation pressure governs the pitch attitude. A bang-bang control law with linear displacement and velocity sensitive switching functions is employed and analytical solutions for the control variables obtained. The nonlinear, nonautonomous, coupled equations of motion are analyzed numerically and the response data presented as functions of system parameters in the form of optimization plots for the controller gain. Versatility of the control system in achieving any arbitrary orientation is demonstrated. An illustrative example towards the end presents results on the expected performance of Anik and the proposed Canadian Communications Technology Satellite (CTS) by simulating their inertia properties in conjunction with the proposed controller.

Formulation of the Problem and Controller Configuration

Equations of Motion

Figure 1 shows an axisymmetric ($I_y = I_z$) satellite with the center of mass S moving in a Keplerian orbit about the center of force O. The satellite consists of a central body I, spinning at a constant average angular velocity, connected to a stabilized platform II through a viscous damper effective in axial rotation. The spatial orientation of the axis of symmetry is completely specified by two successive rotations γ and β, referred to as roll and yaw, respectively, which define the attitude of the satellite principal axes x, y, z with respect to the inertial reference frame x', y', z'. The rotor and the platform spin in the x, y, z reference with angular velocities $\dot{\alpha}$ and $\dot{\lambda}$, respectively.

α being a cyclic coordinate, a first integral of motion defining $\dot{\alpha}$ is given by

$$\dot{\alpha} - \dot{\gamma}\sin\beta + \dot{\theta}\cos\beta\cos\gamma = h_\alpha \tag{1}$$

Since h_α is a measure of the rotor spin, a dimensionless spin parameter, σ defined as

$$\sigma = (\dot{\alpha}/\dot{\theta})|_{\theta=\beta=\gamma=0} = (h_\alpha/\dot{\theta})|_{\theta=0} - 1 \tag{2}$$

may be used to eliminate the cyclic coordinate α.

Neglecting orbital perturbations due to the librational motion and changing the independent variable from t to θ through the use of the Keplerian orbital relations, the classical Lagrangian formulation yields the governing equations of motion in the γ, β, and λ degrees of freedom as[10]:

$$\gamma'' - 2\beta'(\gamma'\tan\beta - \cos\gamma) - (\beta' - \sin\gamma)\sec\beta \times [(1-J)I(\sigma+1)\{(1+e)/(1+e\cos\theta)\}^2 + JI(\lambda' - \gamma'\sin\beta + \cos\beta\cos\gamma)] + \{3(I-1)/(1+e\cos\theta) - 1\}\sin\gamma\cos\gamma - \{2e\sin\theta/(1+e\cos\theta)\}(\gamma' + \cos\gamma\tan\beta) = Q_\gamma \tag{3a}$$

$$\beta'' - \gamma'\cos\gamma - \{2e\sin\theta/(1+e\cos\theta)\}(\beta' - \sin\gamma) + (\gamma'\cos\beta + \cos\gamma\sin\beta)[(1-J)I(\sigma+1)\{(1+e)/(1+e\cos\theta)\}^2 + JI(\lambda' - \gamma'\sin\beta + \cos\beta\cos\gamma) + (\gamma'\sin\beta - \cos\beta\cos\gamma)] - 3\{(I-1)/(1+e\cos\theta)\}\sin^2\gamma\sin\beta\cos\beta = Q_\beta \tag{3b}$$

$$\lambda'' - \gamma''\sin\beta - \{2e\sin\theta/(1+e\cos\theta)\}(\lambda' - \gamma'\sin\beta + \cos\beta\cos\gamma) - \beta'\gamma'\cos\beta - \gamma'\cos\beta\sin\gamma - \beta'\cos\gamma\sin\beta + (K/JI)\{(1+e)^{3/2}/(1+e\cos\theta)^2\}[\lambda' - \gamma'\sin\beta + \cos\beta\cos\gamma - (\sigma+1)\{(1+e)/(1+e\cos\theta)\}^2] = Q_\lambda \tag{3c}$$

These highly nonlinear, nonautonomous, coupled equations of motion do not possess any known closed form solution. One is, therefore, forced to resort to a numerical approach to gain some appreciation as to the system performance.

Magnetic Roll-Yaw Control

Consider a single dipole onboard the platform with an arbitrary orientation $\bar{p}$, strength h^2, and polarity U. The moment generated by interaction with the Earth's magnetic field is then given by,

$$\bar{M} = \bar{P} \times \bar{B} = Uh^2\bar{p} \times \bar{B} \tag{4}$$

Expressing the unit vector $\bar{p}$ and the geomagnetic induction vector $\bar{B}$ in terms of their components along the xyz-axes and using the principle of virtual work, the generalized forces in the roll, yaw, and pitch degrees of freedom can be written as:

$$Q_\gamma = UC_m(p_i B_j - p_j B_i)\sec\beta/(1 + e\cos\theta) \tag{5a}$$

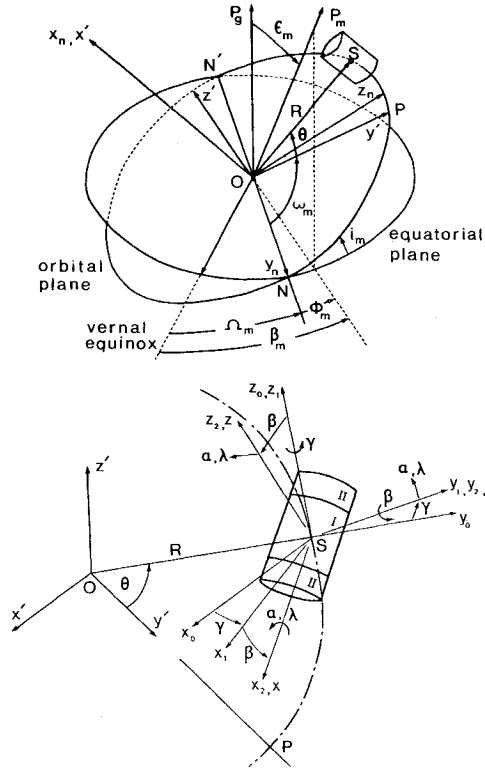

Fig. 1 Geometry of motion.

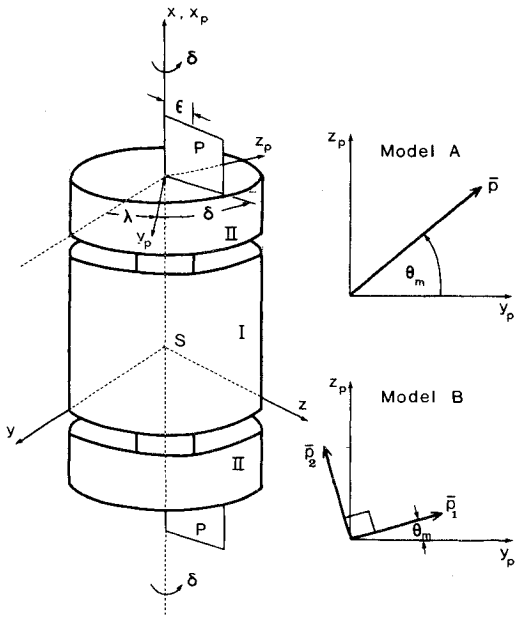

Fig. 2 Controller configurations.

$$Q_\beta = UC_m(p_k B_i - p_i B_k)/(1+e\cos\theta) \tag{5b}$$

$$Q_\lambda{}^m = U(C_m/JI)(p_j B_k - p_k B_j)/(1+e\cos\theta) \tag{5c}$$

where the magnetic parameter C_m, characterizing the magnitude of the magnetically generated moments, is defined as,

$$C_m = h^2 M_e/\mu I_y \tag{6}$$

The body components of $\bar{B}/D_m$ are given by the relations

$$\begin{pmatrix} B_i \\ B_j \\ B_k \end{pmatrix} = \begin{pmatrix} \cos\beta\cos\gamma & \cos\beta\sin\gamma\cos\eta_m + \sin\beta\sin\eta_m & \cos\beta\sin\gamma\sin\eta_m - \sin\beta\cos\eta_m \\ -\sin\gamma & \cos\gamma\cos\eta_m & \cos\gamma\sin\eta_m \\ \sin\beta\cos\gamma & \sin\beta\sin\gamma\cos\eta_m - \cos\beta\sin\eta_m & \sin\beta\sin\gamma\sin\eta_m + \cos\beta\cos\eta_m \end{pmatrix} \begin{pmatrix} B_{xn} \\ B_{yn} \\ B_{zn} \end{pmatrix} \tag{7}$$

The geomagnetic induction components along the orbit normal, ascending node and perpendicular to the line of nodes in the orbital plane are well established.[11] For an Earth-centered canted dipole model, they are:

$$B_{xn} = -\cos i_m\cos\varepsilon_m + \sin i_m\sin\varepsilon_m\sin\phi_m \tag{8a}$$

$$B_{yn} = (3/2)\sin i_m\sin 2\eta_m\cos\varepsilon_m + (1/2)[\cos\phi_m + (3/2)\{(1+\cos i_m)\cos(2\eta_m-\phi_m) + (1-\cos i_m)\times\cos(2\eta_m+\phi_m)\}]\sin\varepsilon_m \tag{8b}$$

$$B_{zn} = (1/2)\sin i_m(1-3\cos 2\eta_m)\cos\varepsilon_m + (1/2)[\cos i_m\times\sin\phi_m + (3/2)\{(1+\cos i_m)\sin(2\eta_m-\phi_m) + (1-\cos i_m)\sin(2\eta_m+\phi_m)\}]\sin\varepsilon_m \tag{8c}$$

It may be pointed out here that the angle ϕ_m varies due to the Earth's rotation and the regression of the line of nodes, according to $\phi_m = (n_e + n_r)$. Its governing equation with the orbital angle as the independent variable is

$$\phi_m' = (n_e+n_r)(R_p{}^3/\mu)^{1/2}(1+e)^{3/2}/(1+e\cos\theta)^2 \tag{9}$$

which has the solution (for $e<1$)

$$\phi_m = \phi_{mo} + \{(n_e+n_r)(R_p{}^3/\mu)^{1/2}(1+e)^{3/2}/(1-e^2)\}\times[-e\sin\theta/(1+e\cos\theta) + \{2/(1-e^2)^{1/2}\}\times\tan^{-1}\{(1-e)^{1/2}\tan(\theta/2)/(1+e)^{1/2}\}] \tag{10}$$

where the appropriate quadrant for the arctan function is to be introduced. The present analysis ignores the nodal regression as a dynamic effect which is equivalent to assuming the Earth to be gravitationally spherical.

For controlling satellite nutations in an equatorial orbit with the nominal position of the spin axis along the orbit normal, it can be easily shown that the maximum transverse torque, $(Q_\gamma{}^2\cos^2\beta + Q_\beta{}^2)^{1/2}$, results when $p_i = 0$. Accordingly, two magnetic controller models with dipoles in the satellite's transverse plane are considered here (Fig. 2).

Model A consists of a single dipole rotatable about the x_p axis in the platform fixed reference x_p, y_p, z_p. Physically, it would correspond to a single electromagnet rotating about the axis of symmetry or two (or more) fixed electromagnets with variable currents. The moments generated are given by

$$Q_\gamma = -UC_m p_j B_i \sec\beta/(1+e\cos\theta) \tag{11a}$$

$$Q_\beta = UC_m p_k B_i/(1+e\cos\theta) \tag{11b}$$

$$Q_\lambda{}^m = U(C_m/JI)(p_j B_k - p_k B_j)/(1+e\cos\theta) \tag{11c}$$

where

$$p_j = \cos(\theta_m+\lambda), \qquad p_k = \sin(\theta_m+\lambda)$$

A constant dipole level h^2, leading to a constant value of the magnetic parameter C_m, is assumed in the present analysis. The components of the total transverse torque are controlled according to the relations:

$$\operatorname{sgn}(Q_\gamma\cos\beta) = -\operatorname{sgn} S_\gamma \tag{12a}$$

$$\operatorname{sgn} Q_\beta = -\operatorname{sgn} S_\beta \tag{12b}$$

$$Q_\gamma\cos\beta/Q_\beta = S_\gamma/S_\beta \tag{12c}$$

where the switching functions $S_i (i = \gamma, \beta)$ are defined as

$$S_i = i' + m(i - i_f), \qquad i = \gamma, \beta \tag{13}$$

and the controller gain m is chosen according to some suitable criterion, such as, the least time of damping or the maximum permissible displacement during a nutation cycle.

This results in a simple control law for the dipole angle θ_m (Fig. 2)

$$\theta_m = -\lambda - \tan^{-1}(S_\beta/S_\gamma) \tag{14}$$

Note that no polarity reversals are required if the angle θ_m is permitted any value in the range 0 to 2π. However, it would be desirable to restrict θ_m to the range $-\pi/2$ to $\pi/2$ (for the gimballed electromagnet) and permit polarity reversals, which leads to the controls:

$$\theta_m = -\tan^{-1}\{(S_\beta + S_\gamma\tan\lambda)/(S_\gamma - S_\beta\tan\lambda)\} \tag{15a}$$

$$U = \operatorname{sgn}\{(S_\gamma\cos\lambda - S_\beta\sin\lambda)/B_i\} \tag{15b}$$

where the principal value of the arctan function is to be admitted.

Model B consists of two mutually perpendicular dipoles with orientations $\bar{p}_1$ and $\bar{p}_2$ fixed in the platform and allowed polarity reversals (Fig. 2). Substituting for the unit vectors $\bar{p}_1$ and $\bar{p}_2$ in Eqs. (5), the magnetic control moments become

$$Q_\gamma = -(U_1 p_{1j} + U_2 p_{2j})C_m B_i \sec\beta/(1+e\cos\theta) \tag{16a}$$

$$Q_\beta = (U_1 p_{1k} + U_2 p_{2k})C_m B_i/(1+e\cos\theta) \tag{16b}$$

$$Q_\lambda{}^m = \{U_1(p_{1j}B_k - p_{1k}B_j) + U_2(p_{2j}B_k - p_{2k}B_j)\}(C_m/JI)/(1+e\cos\theta) \tag{16c}$$

where

$$p_{1j} = p_{2k} = \cos(\theta_m+\lambda), \qquad p_{1k} = -p_{2j} = \sin(\theta_m+\lambda)$$

Although the bang-bang controller can no longer distribute the total transverse moment between the roll and yaw degrees of freedom in proportion to the demands governed by the switching functions, appropriate signs of Q_γ and Q_β may be achieved with the polarity controls:

for $|\tan(\theta_m+\lambda)| < 1$,

$$U_1 = \operatorname{sgn}\{S_\gamma/B_i\cos(\theta_m+\lambda)\}$$

$$U_2 = -\operatorname{sgn}\{S_\beta/B_i\cos(\theta_m+\lambda)\} \tag{17a}$$

for $|\tan(\theta_m+\lambda)| > 1$,

$$U_1 = -\operatorname{sgn}\{S_\beta/B_i\sin(\theta_m+\lambda)\}$$

$$U_2 = \operatorname{sgn}\{S_\gamma/B_i\sin(\theta_m+\lambda)\} \tag{17b}$$

Note that θ_m defining the locations of the dipoles with respect to the platform fixed axes is a constant in this case. For the final pitch orientation $\lambda_f = 0$ (the axis y_p pointing towards the Earth), the minimum cancellation of the torques due to the two

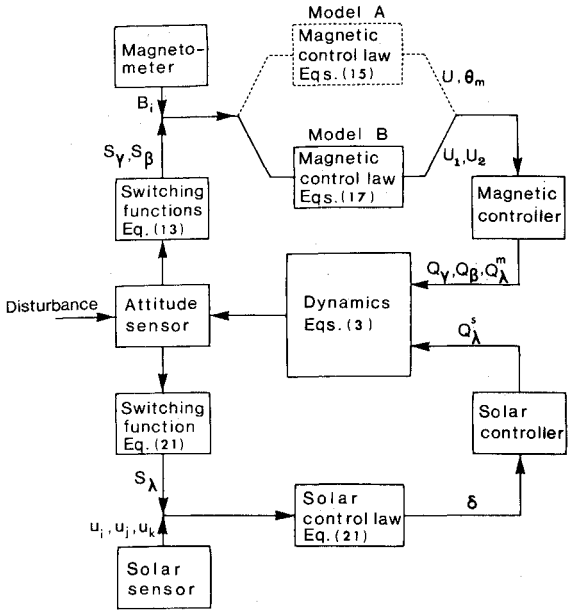

Fig. 3 Control flow diagram.

dipoles occurs when $\theta_m = 0$. Furthermore, for most applications requiring $-\pi/4 < \lambda < \pi/4$, the controls reduce to:

$$U_1 = \text{sgn}(S_\gamma/B_i), \qquad U_2 = \text{sgn}(S_\beta/B_i) \tag{18}$$

Solar Pitch Control

One major limitation of a magnetic system is its inability to provide first-order pitch control torques for satellites in near-equatorial orbits. This, of course, is due to the geomagnetic field being nearly parallel to the orbit normal. The pitch degree of freedom, on the other hand, would be subject to disturbances, external as well as those resulting from the operation of the roll-yaw magnetic controller [Eqs. (11c) and (16c)]. A need for a pitch controller is thus apparent. Although this is normally accomplished through an active device in practice, there is an interesting possibility of achieving pitch control in a semi-passive manner using solar radiation pressure.

The proposed solar pitch controller consists of plates PP which are allowed a rotation δ about the axis of symmetry of the satellite (Fig. 2). For highly reflective plates, the pure pitch moment resulting from solar radiation pressure is found to be,[8]

$$Q_\lambda{}^s = -C\{(1+e)^3/(1+e\cos\theta)^4\}\,|-u_j\sin(\delta+\lambda)+ u_k\cos(\delta+\lambda)|\{-u_j\sin(\delta+\lambda)+u_k\cos(\delta+\lambda)\} \tag{19}$$

where the solar parameter C is defined as:

$$C = (2\rho p_o R_p{}^3/\mu I_{xp})A\varepsilon \tag{20}$$

Using the control relation $Q_\lambda{}^s = -|Q_\lambda{}^s|_{\max}\,\text{sgn}\,S_\lambda$ with the switching function $S_\lambda = \lambda' + m(\lambda - \lambda_f)$, the control law for the plate rotation δ becomes:

for $u_j > 0$,

$$\delta = \tan^{-1}(u_k/u_j) - \lambda - (\pi/2)\,\text{sgn}\,S_\lambda$$

for $u_j < 0$,

$$\delta = \pi + \tan^{-1}(u_k/u_j) - \lambda - (\pi/2)\,\text{sgn}\,S_\lambda$$

for $u_j = 0$,

$$\delta = \cos^{-1}\{-\text{sgn}(u_k S_\lambda)\} \tag{21}$$

where the principal value of the arctan function is to be introduced.

The total generalized force in the pitch degree of freedom is then given by,

$$Q_\lambda = Q_\lambda{}^m + Q_\lambda{}^s \tag{22}$$

It may be pointed out here that the components of the unit vector in the direction of the sun involve orbital parameters Ω, i, and ω referred to the ecliptic plane while the formulation of the magnetic controller requires the same angles referred to the Earth's equatorial plane. The relations governing these parameters for an arbitrary orbital plane are readily obtained as:

$$\begin{aligned}
\sin\Omega_m \sin i_m &= \sin\Omega \sin i \\
\cos\Omega_m \cos\omega_m - \sin\Omega_m \sin\omega_m \cos i_m &= \cos\Omega\cos\omega - \\
&\quad \sin\Omega\sin\omega\cos i \\
\cos\Omega_m \sin\omega_m + \sin\Omega_m \cos\omega_m \cos i_m &= \cos\Omega\sin\omega + \\
&\quad \sin\Omega\cos\omega\cos i
\end{aligned} \tag{23}$$

Figure 3 synthesizes the various steps involved in the control strategy. The equations governing the individual blocks are indicated in the figure to facilitate appreciation of the mathematical development.

Results and Discussion

The response of the system was studied by numerically integrating the equations of motion (3) along with the control relations governing the magnetic and solar generalized forces, i.e., Eqs. (11, 15, 21, and 22) and Eqs. (16, 17, 21, and 22) for models A and B, respectively. The Adams-Bashforth predictor-corrector quadrature with the Runge-Kutta starter was used with a step size of 0.1° which gave results of sufficient accuracy. The amount of information generated is rather extensive; however, for conciseness, only the typical results sufficient to establish trends are presented here. In general, the system is exposed to extremely severe disturbances, much higher than it is likely to encounter in the normal operation, to evaluate the controller's performance under adverse conditions.

Nutation Damping

Figure 4 summarizes the performance of the proposed magnetic-solar hybrid controller in damping the nutational motion of the satellite spin axis and the pitch oscillation of the platform. It shows the variation of the damping time τ_d with

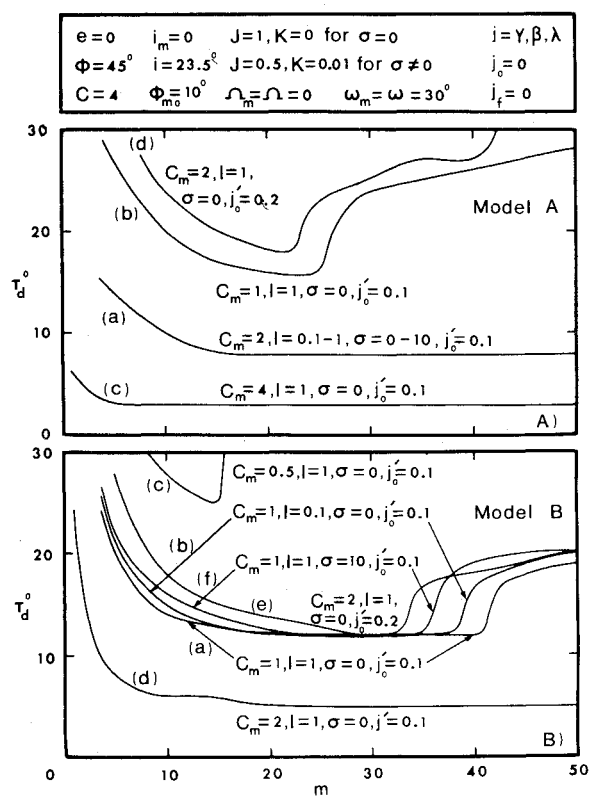

Fig. 4 Optimization plots for controller gain.

the controller gain m for a variety of combinations of the system parameters and initial conditions. Here the damping time is defined as the time required for all the three degrees of freedom; namely, the roll γ, yaw β, and the platform pitch λ, to settle within 0.1° of the desired final orientation. The responses of both magnetic controller models A and B are presented which, in general, indicate the existence of an optimum value of the system gain m leading to the minimum time of damping, and the sensitivity of the optimum to the system parameters and initial conditions.

The influence of the satellite inertia and spin parameters on the attitude dynamics of passively stabilized satellites is well recognized. Their effect on the nutation damping performance of the present controlled system, however, appears to be negligible. This is indicated by curve (a) in Fig. 4A where the results for pencil-like to spherical mass distributions ($I = 0.1$ to 1) and nonspinning to moderate spin rates ($\sigma = 0$ to 10) were virtually indistinguishable. The banding together of curves a, b, and f in Fig. 4B reflects similar system behavior. The insensitivity of the transient response to I and moderate values of σ is understandable as these parameters, contributing restoring forces to the system, are now largely provided for by the controller gain m. The performance under high spin rates is investigated in a later section.

The effect of the magnetic parameter C_m, characterizing the magnitude of the magnetic control torques, is indicated by a comparison of curves a–c in Fig. 4A for the case of the single rotatable dipole. As anticipated, increasing the value of C_m leads to a corresponding reduction in the damping time τ_d. Larger values of the magnetic parameter (curves a and c) show a response pattern that is relatively insensitive to the controller gain m, thus indicating a large range of values of the latter to provide near-optimum damping. It may, however, be pointed out that the maximum attainable value of C_m is subject to constraints imposed by the electromagnet weight and power requirement.

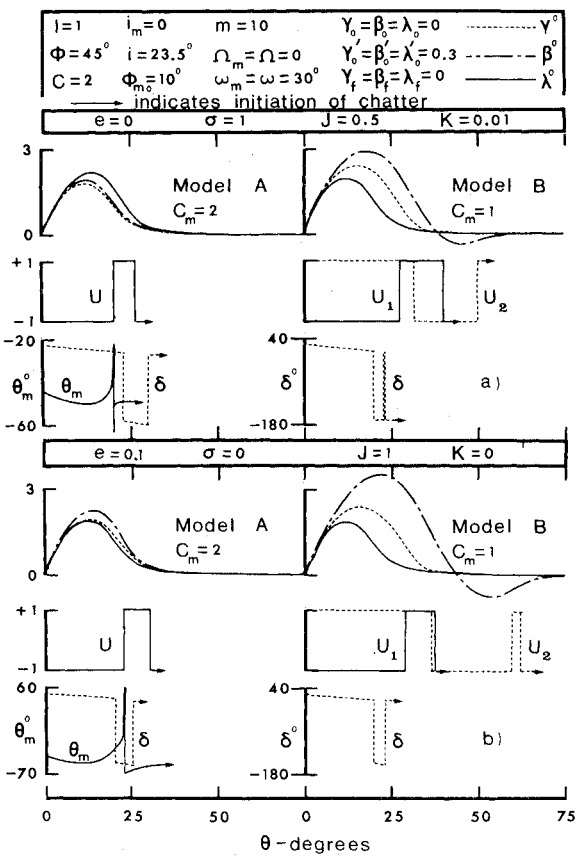

Fig. 5 Damped response and time history of controls subsequent to initial impulsive disturbance.

Curves c, a, and d indicate similar effect of the magnetic parameter for the model with two fixed transverse dipoles (Fig. 4B). A comment concerning the influence of the solar parameter would be appropriate here. An increased value of C led to a reduced damping time for the pitch (λ) degree of freedom. However, even with a value of $C = 2$, it was found that the pitch oscillation damped out faster than the roll-yaw motion, except for the case of large viscous drags on the platform (large K, σ).

A comparison of curves a and d in Fig. 4A and curves d and e in Fig. 4B shows the effect of initial conditions on the performance of controller models A and B, respectively. In both cases, an increased impulsive disturbance not only leads to an anticipated increase in the damping time but also renders the response quite sensitive to the system gain m. With larger values of C_m, however, the latter effect was found to be less pronounced.

It is of interest to compare the performance of the two magnetic controller models in damping the attitude motion. A suitable criterion for the comparison is the same total electromagnet weight and power consumption which requires the value of the magnetic parameter C_m for model A to be twice the value for model B. Comparisons may be made of curves b, a, and c in Fig. 4A with curves c, a, and d in Fig. 4B, respectively, towards this end. The results clearly indicate a better performance of the single rotatable dipole model A. This is explained by the ability of this model to distribute the total magnetic torque between the roll and yaw degrees of freedom in proportion to their demands determined here by the switching functions S_γ and S_β, respectively.

The single rotating dipole model A may be obtained by using a rotating electromagnet, which, however, would involve additional weight and power requirement for the turning mechanism and a reduction in the system reliability due to physical movement of the electromagnet. Alternately, two fixed electromagnets with variable currents may be employed. Unfortunately, this would require each electromagnet to be the same size as the single rotating one in order to maintain the same resultant dipole strength as the latter, thus doubling the total weight. The choice between the physical arrangements leading to model A or B would be governed by such mission oriented factors as the system reliability, associated hardware and software, and performance requirements.

Typical damped responses of a satellite subjected to an extremely severe impulsive disturbance are shown in Fig. 5 for both controller models. The time history of the controls is also included. Figure 5a shows the response in a circular orbit with a nominal value of $\sigma = 1$, which may be required from such considerations as temperature control. The damped attitude motion of a nonspinning satellite in an eccentric orbit is shown in Fig. 5b, which indicates a slight increase in the maximum amplitude and the damping time. The effectiveness of the controllers in damping such a severe impulsive disturbance in a few degrees of the satellite's orbital travel is thus apparent. The amplitudes are also limited to a few degrees. The controls, in general, require rather infrequent switching until the corresponding amplitudes become very small and chatter initiates. This may, however, be prevented by the inclusion of suitable deadbands in the control relations which would depend on the pointing accuracies required.

The effectiveness of the control system in capturing a satellite from initial roll, yaw, and pitch errors is presented in Fig. 6 Both circular and eccentric orbit as well as nonspinning and moderate spin rate cases are considered. The initial error of 20° in each degree of freedom is corrected in approximately one-third of an orbit with model A and half an orbit with model B. The performance may be improved further through an optimum choice of the controller gain.

High Spin Rates and Spin Decay

The discussion so far establishes the effectiveness of the control system for satellites which are either nonspinning or have

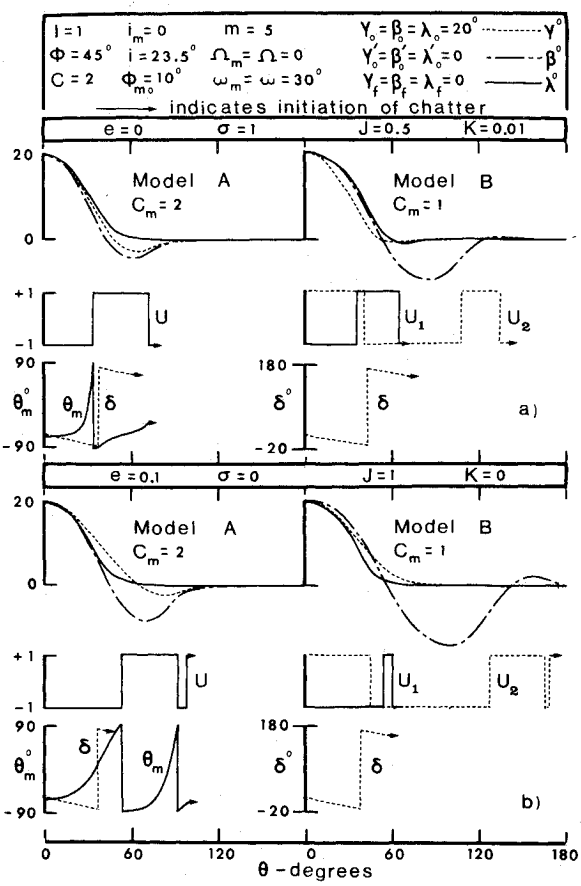

Fig. 6 Damped response and time history of controls subsequent to initial position disturbance.

moderate spin rates. A study of the response characteristics of the system with high spin rates would be of interest as several configurations in practice utilize a high speed rotor. The response of satellites with high spin rates in conjunction with the controller (model B) is indicated by the data presented in Table 1, which shows the coning amplitude of the spin axis, Φ_{max}, and the damping time τ_d. The coning amplitude Φ_{max} reached in the absence of the controller is also presented. For low spin rates, the control system, in addition to providing nutation damping, helps keep the amplitudes low. However, for high spin rates, it essentially acts as a damper. A comparison of the controller

Table 1 Response with high spin rates

$e=0$	$I=1.2$	$i_m=0$	$\Omega_m=\Omega=0$	$\gamma_o=\beta_o=\lambda_o=0$
$J=0.5$	$\phi=45°$	$i=23.5°$	$\omega_m=\omega=30°$	$\gamma_o'=\beta_o'=0.3$
$K=0$	$C=4$	$\phi_{mo}=10°$	$\lambda_o'=0$	$\gamma_f=\beta_f=\lambda_f=0$

	$C_m=2$	$m=10$	$C_m=2$	$m=30$	$C_m=0$
σ	$\Phi_{max}°$	$\tau_d°$	$\Phi_{max}°$	$\tau_d°$	$\Phi_{max}°$
0	1.86	28.20	1.86	29.50	39.88
10	1.78	28.26	1.77	30.86	6.61
25	1.61	26.04	1.53	34.56	2.99
35	1.39	30.96	1.34	43.56	2.19
50	1.12	24.22	1.10	25.50	1.56
75	0.84	21.84	0.84	35.56	1.05
100	0.67	19.44	0.67	33.88	0.79
200	0.37	15.54	0.37	22.26	0.40
300	0.25	11.82	0.25	13.20	0.27
400	0.19	9.70	0.19	9.78	0.20
500	0.16	6.68	0.16	6.66	0.16
600	0.13	4.50	0.13	4.52	0.13

performance with $m=10$ and $m=30$ shows its effect on the amplitude to be slight but the damping time is affected appreciably up to spin parameter values as high as $\sigma=200$. These observations substantiate the earlier conclusion regarding the controller gain lending stiffness to the system. For still higher spin rates ($\sigma>200$), however, the influence of m is negligible indicating the dominance of the gyroscopic restoring forces.

The analysis so far considered the rotor to have a constant average spin rate. Apparently this would be achieved through some active energy source compensating for rotor spin decay due to bearing losses. Even in the absence of such energy supply, the analysis continues to be valid provided the spin parameter σ remains sensibly invariant over a time interval of the order of the damping times attained here. This is of considerable value as any spin decay is likely to occur very slowly indeed. Thus the data presented in Table 1 can also be used to predict the long-range performance of a spinning satellite.

The foregoing emphasizes the fact that, in the presence of the proposed control system, it is no longer necessary to spin the satellite for attitude stabilization. The inclusion of the spinning rotor, however, does reduce the maximum coning angle and the damping time.

Attitude Control

The control system offers the exciting possibility of stabilizing the satellite along any arbitrary orientation in space, thus enabling it to undertake diverse missions. This may be achieved through the parameters γ_f, β_f, and λ_f, defining the final desired orientation, which are incorporated in the switching functions S_γ, S_β, and S_λ, respectively. Figure 7 shows the ability of the controller in achieving a variety of spatial orientations, the time taken being well within an orbit. Note that a fairly small value of the gain m used here leads to a smooth transition between widely different attitudes. On the other hand, larger values of m were found to result in an undesirable overshoot of the final orientation. It may be pointed out further that

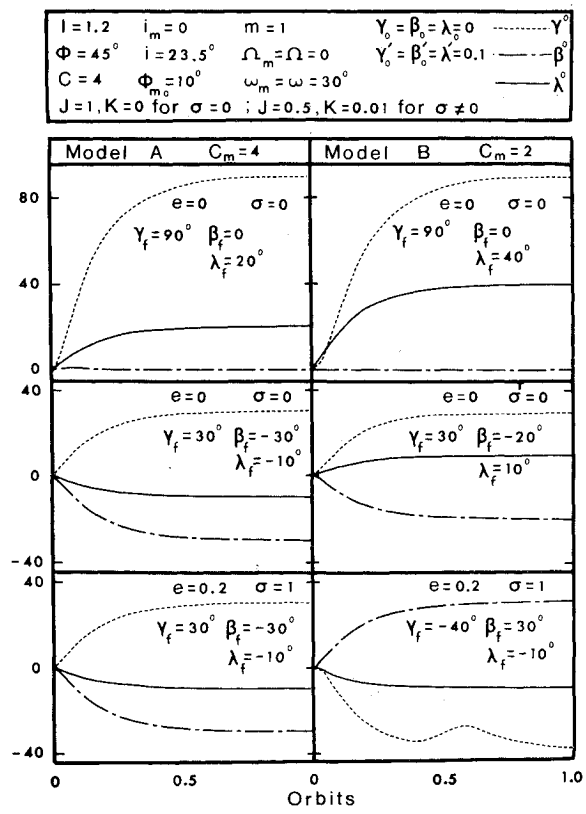

Fig. 7 Effectiveness of the controller in imparting arbitrary orientations to the satellite.

except for final orientations along equilibrium points of the system, the controller must at all times provide corrective torques to counter the gravity gradient and gyroscopic moments. Moderate values of the magnetic parameter taken here, $C_m = 4$ for model A and $C_m = 2$ for model B, are found to be sufficient for both nonspinning and a nominal spin rate in circular as well as elliptic orbits of eccentricity $e = 0.2$ (Fig. 7).

Illustrative Example

In order to gain a better appreciation of the controller performance, the projected response using inertia properties of two typical communications satellites—the proposed Canadian Communications Technology Satellite (CTS) and Anik—were evaluated. For convenience the latter may be considered as nonspinning which only represents an adverse situation. Values of the magnetic parameter $C_m = 4$ for model A and $C_m = 2$ for model B are attainable with total dipole levels of approximately 200 and 20 amp-m^2 for the CTS and Anik, respectively. A total control plate area $A = 1$ ft^2 and moment arm $\varepsilon = 5$ ft yields a solar parameter value of $C \simeq 2$. On the other hand, pitch control may be achieved using a reaction wheel of capacity $\simeq$ 0.1 lb-ft-sec/day which is equivalent to $C = 2$. An impulsive disturbance of 0.1 is applied in all the three degrees of freedom simultaneously which is in excess of that imparted by micrometeorite impacts over 24 hrs,[8,12] and thus represents an enormous magnification of the real situation. As the inertia parameter ($I \simeq 0.1$ for CTS, 1 for Anik) did not affect the performance significantly, most of the results presented in this paper are representative of these satellites. It is apparent from Fig. 4 that the controllers are able to damp such a severe disturbance in about 3° and 5° of the orbit with models A and B, respectively. The maximum deviation from the orbit normal attitude also remained less than 0.2°. Any arbitrary orientations may be imparted to the satellites in well within an orbital period (Fig. 7).

Finally, a comment concerning the Earth's shadow, which would render the solar pitch controller ineffective, is appropriate here. For a geo-stationary orbit, the influence of shadow is confined to a quarter of the satellite's lifespan and even here, only during 5% of the orbital period. This would imply a maximum eclipse period of about 1.2 hrs. Although the magnetic roll-yaw control remains unaffected by the shadow, the disturbances experienced during this time would lead to a buildup of the pitch attitude error. On emergence from the shadow the controller would tend to arrest this trend and correct it over a period of time governed by the magnitude of the error.

Furthermore, it should be pointed out that the analysis ignores dynamics due to relative motion of the gimballed electromagnet (model A) and the solar control plates, possible shadowing of the latter by the satellite, and interaction effects due to residual spacecraft dipole. For a given satellite with a specified controller these effects can easily be incorporated in the analysis, however, for any configuration of practical significance their influence on the controller's performance is likely to be of little consequence.

Conclusions

The significant conclusions based on the analysis may be summarized as follows:

1) The feasibility of a magnetic-solar hybrid controller for nutation damping and attitude control of satellites in equatorial orbits is clearly demonstrated. Although not presented here for conciseness, the results suggest that the controller performance does not deteriorate substantially for eccentric orbits ($e < 0.5$) and orbital inclinations ($i_m < 60°$). In fact, for altitudes down to 500 miles (boundary of the Earth's atmosphere), the controller's performance showed improvement in terms of real damping time.

2) The analysis permits interchangeability of the solar controller and a variable speed pitch momentum wheel, thus effectively describing a gyromagnetic control system.

3) The ability of the system in damping extremely severe disturbances in a few degrees of the orbit makes it quite suitable for applications, such as communications, etc.

4) Even with rotor spin decay, the system continues to function effectively which promises an increased satellite lifespan.

5) It is possible for a satellite to attain any arbitrary orientation in space, both in circular and elliptic orbits. The controller thus imparts versatility to a space vehicle in undertaking diverse missions.

6) The pitch controller becomes ineffective when the satellite is in the Earth's shadow. Even in the worst situation the loss of control corresponds to only 1.2 hr per orbit for geostationary satellites. However, for about 75% of its lifetime, the geostationary orbit is entirely free of the Earth's shadow.

References

[1] Wheeler, P. C., "Spinning Spacecraft Attitude Control via the Environmental Magnetic Field," *Journal of Spacecraft and Rockets*, Vol. 4, No. 12, Dec. 1967, pp. 1631–1637.

[2] Hecht, E. and Manger, W. P., "Magnetic Attitude Control of the TIROS Satellites," *Torques and Attitude Sensing in Earth Satellites*, edited by S. F. Singer, Academic Press, New York, 1964, pp. 127–135.

[3] Lindorfer, W. and Muhlfelder, L., "Attitude and Spin Control for TIROS Wheel," *AIAA/JACC Guidance and Control Conference*, Seattle, Wash., 1966, pp. 448–461.

[4] Shigehara, M., "Geometric Attitude Control of an Axisymmetric Spinning Satellite," *Journal of Spacecraft and Rockets*, Vol. 9, No. 6, June 1972, pp. 391–398.

[5] Bainum, P. M. and Mackison, D. L., "Gravity-Gradient Stabilization of Synchronous Orbiting Satellites," *Journal of the British Interplanetary Society*, Vol. 21, 1968, pp. 341–369.

[6] Modi, V. J. and Tschann, C., "On the Attitude and Librational Control of a Satellite using Solar Radiation Pressure," *Astronautical Research 1970, Proceedings of the XXI Congress of the International Astronautical Federation*, edited by L. G. Napolitano, North-Holland Publishing Co., Amsterdam, 1971, pp. 84–100.

[7] Modi, V. J. and Kumar, K., "Coupled Librational Dynamics and Attitude Control of Satellites in Presence of Solar Radiation Pressure," *Astronautical Research 1971, Proceedings of the XXII Congress of the International Astronautical Federation*, edited by L. G. Napolitano, D. Reidel Publisher, Dordrecht, the Netherlands, pp. 37–52.

[8] Modi, V. J. and Pande, K. C., "Solar Pressure Control of a Dual-Spin Satellite," *Journal of Spacecraft and Rockets*, Vol. 10, No. 6, June 1973, pp. 355–361.

[9] Scull, J. R., "Mariner IV Revisited, or the Tale of the Ancient Mariner," presented at the *20th Congress of the International Astronautical Federation*, Argentina, Oct. 1969.

[10] Pande, K. C., "Attitude Control of Spinning Satellites using Environmental Forces," Ph.D. thesis, Department of Mechanical Engineering, University of British Columbia, Vancouver, Canada, Nov. 1973, pp. 55–59.

[11] RCA, "RCA Flywheel Stabilized, Magnetically Torqued Attitude Control System for Meteorological Satellites," CR-232, 1965, NASA.

[12] Ehricke, K. A., *Principles of Guided Missile Design*, Van Nostrand, N.J., 1960, pp. 241–256.